Biochemistry

Communication

pubs.acs.org/biochemistry

Avidity for Polypeptide Binding by Nucleotide-Bound Hsp104 Structures

Clarissa L. Weaver,[†] Elizabeth C. Duran,[†] Korrie L. Mack,[‡] JiaBei Lin,[‡] Meredith E. Jackrel,[‡] Elizabeth A. Sweeny,[‡] James Shorter,[‡] and Aaron L. Lucius*[,†]

[†]Department of Chemistry, University of Alabama at Birmingham, Birmingham, Alabama 35294, United States

[‡]Department of Biochemistry and Biophysics, Perelman School of Medicine, University of Pennsylvania, Philadelphia, Pennsylvania 19104, United States

Supporting Information

ABSTRACT: Recent Hsp104 structural studies have reported both planar and helical models of the hexameric structure. The conformation of Hsp104 monomers within the hexamer is affected by nucleotide ligation. After nucleotide-driven hexamer formation, Hsp104-catalyzed disruption of protein aggregates requires binding to the peptide substrate. Here, we examine the oligomeric state of Hsp104 and its peptide binding competency in the absence of nucleotide and in the presence of ADP, ATPγS, AMPPNP, or AMPPCP. Surprisingly, we found that only ATPγS facilitates avid peptide binding by Hsp104. We propose that the modulation between high- and low-peptide affinity states observed with these ATP analogues is an important component of the disaggregation mechanism of Hsp104.

Saccharomyces cerevisiae Hsp104 is a member of the Hsp100 (heat shock protein) family of AAA+ (ATPases associated with diverse cellular activities) motor proteins that function broadly to help organisms survive and adapt to environmental stress.[1,2] Accumulation of unfolded or misfolded proteins into aggregates can occur when protein homeostasis systems are overwhelmed. Hsp104 promotes cell survival by resolving these aggregates.[3] Such aggregation in humans is implicated in neurodegenerative diseases, including Parkinson's disease and amyotrophic lateral sclerosis. Remarkably, no cytoplasmic homologue to Hsp104 exists in humans. Consequently, there is great interest in understanding how Hsp104 resolves protein aggregates, with a vision of developing it for therapeutic applications.[4−6]

Like other members of the Hsp100 family, Hsp104 is biologically active as a hexameric ring but may exist in a dynamic equilibrium of oligomers.[7] ClpB, the *Escherichia coli* homologue of Hsp104 populates a distribution of oligomers, affected by protein concentration, salt concentration, and ligand (nucleotide).[8,9] The nonhydrolyzable ATP analogue β,γ-imidoadenosine 5′-triphosphate (AMPPNP) was used to populate hexamers for crystallographic and cryo-electron microscopy studies of *Thermus thermophilus* ClpB (*T*ClpB).[10,11] While ClpB is structurally similar to Hsp104 and both proteins function to resolve amorphous protein aggregates, Hsp104 has unique amyloid remodeling[12] and prion propagating[13] activities that ClpB does not share. Furthermore, complementary cochaperones from the prokaryotic and eukaryotic systems are not interchangeable, highlighting a species-specific interface.[14,15] Thus, investigations of Hsp104 provide information that is not available from the investigations of ClpB.

Interestingly, although the biologically active form of these motor proteins is a hexameric ring, Hsp104, ClpB, and closely related AAA+ family member ClpA have crystallized in extended spiral filaments.[10,16,17] In contrast, a study of AAA+ protein ClpC with AMPPNP revealed planar ring hexamers in the crystallographic unit.[18] Many electron microscopy (EM) studies of Hsp104 have also shown planar hexameric rings with a variety of bound nucleotides.[3,17,19−21] The poorly hydrolyzable ATP analogue, adenosine 5′-(3-thiotriphosphate) (ATPγS), and ADP have been used to investigate conformation, oligomerization, and protein remodeling activity of wild-type Hsp104, whereas ATP has been used with Hsp104 variants that are deficient in ATP hydrolysis.[22,23]

Each monomer of Hsp104, ClpB, ClpA, and ClpC has two nucleotide binding and hydrolysis domains that, in most reconstructions and models, form stacked rings in the planar hexamer.[3,10,17−21,24] Monomers adopt different conformations within the ring when unligated or ligated with different nucleotides. These studies led to proposed mechanisms of conformational changes throughout the ATP binding and hydrolysis cycle that are mechanistically linked to disaggregase activity.[19] In contrast to these planar structures, a recent EM study showed Hsp104 bound by AMPPNP in a novel helical hexameric spiral with an asymmetric seam.[25]

Given the abundance of structural models for Hsp104 and the influence of nucleotide binding on conformation, we sought to address the question of whether the oligomers bound by various nucleotides in solution differ structurally and display different polypeptide binding activity.

We have shown that Hsp104 binds FITC-casein in the presence of ATPγS.[5] Previously, Bösl et al. demonstrated that Hsp104 binds to another model substrate (RCMLa) in the presence of ATPγS. ADP did not facilitate polypeptide binding because of the lower affinity of Hsp104 for the polypeptide in the ADP-bound state. Surprisingly, ATP also failed to facilitate peptide binding, because of rapid hydrolysis of ATP resulting in

Received: March 10, 2017
Revised: April 3, 2017
Published: April 5, 2017

ACS Publications © XXXX American Chemical Society

DOI: 10.1021/acs.biochem.7b00225
Biochemistry XXXX, XXX, XXX−XXX

the low-affinity ADP-bound state.[22] Here, we use a polypeptide consisting of the first 50 amino acids of RepA, a soluble substrate used to examine Hsp104 protein remodeling activity.[5,26−29]

We extend our investigation to include AMPPNP, which was used to examine both the *T*ClpB crystal structure and the Hsp104 spiral hexamer. In addition, we include β,γ-methyleneadenosine 5′-triphosphate (AMPPCP), which has been used for structural studies of Hsp104 and *E. coli* ClpB.[10,25,30] Because ATP is rapidly hydrolyzed, resulting in ADP and inorganic phosphate, ATP is not included in this study. We found that only ATPγS promotes the formation of an Hsp104 structure that is competent for stable polypeptide binding under the conditions tested.

As a necessary precursor to investigating peptide binding, we first addressed two questions with respect to the quaternary structure of Hsp104. First, is nucleotide binding required for the formation of hexameric rings of Hsp104? Second, if nucleotide binding is required, which nucleotides can fulfill this role? To address these questions, we performed sedimentation velocity experiments to examine Hsp104 assembly. Experiments were performed on 2 μM Hsp104 in the absence of any nucleotide. Figure 1A shows the resulting $c(s)$ distribution, where multiple peaks are observed, indicating that various oligomeric states are populated in the absence of a nucleotide. However, one peak with an $s_{20,w}$ of ∼16 S dominates the $c(s)$ distribution, suggesting that one oligomeric state is predominantly populated under these conditions.

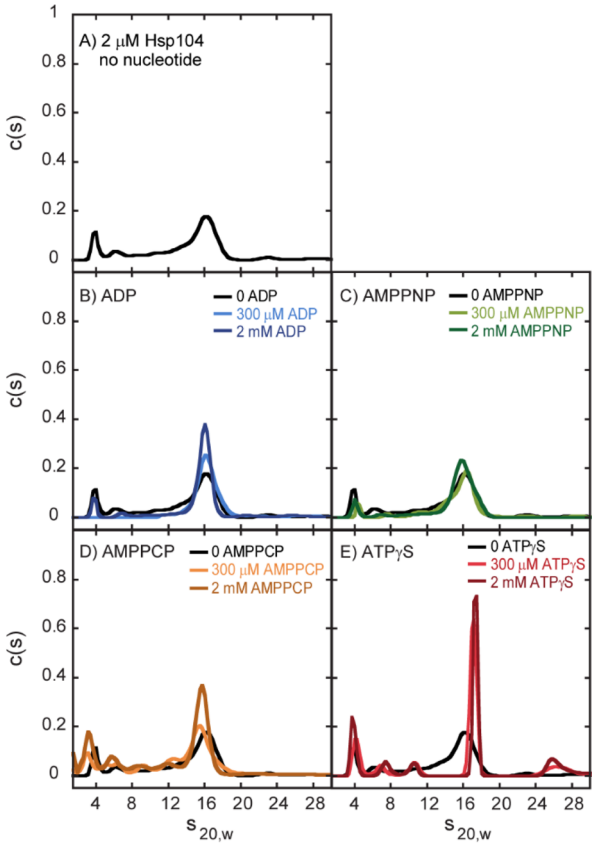

Figure 1. Sedimentation velocity $c(s)$ distributions of Hsp104 in the absence and presence of nucleotides. Sedimentation velocity experiments were performed with 2 μM Hsp104 (A) in the absence and in the presence of (B) ADP, (C) AMPPNP, (D) AMPPCP, or (E) ATPγS.

Experiments were then performed with 2 μM Hsp104 in the presence of 300 μM ADP, AMPPNP, AMPPCP, or ATPγS. Panels B−E of Figure 1 show the resulting $c(s)$ distributions from analysis of the sedimentation boundaries. In all cases, a dominant peak between ∼15.5 and 17 S was observed. Strikingly, the ATPγS-bound structure exhibits a dominant population of oligomers with a sedimentation coefficient that is larger than those of the other nucleotide-bound structures (see Table 1).

Table 1. Hsp104 Predominant $c(s)$ Distributions and Frictional Ratios[a]

condition	$\bar{s}_{20,w}$ (S)	f/f_0
no nucleotide	15.8 ± 0.3	1.35 ± 0.03
ADP	16.1 ± 0.3	1.35 ± 0.02
AMPPNP	15.9 ± 0.1	1.36 ± 0.01
AMPPCP	15.6 ± 0.1	1.39 ± 0.01
ATPγS	17.0 ± 0.2	1.28 ± 0.02

[a]Standard deviation based on the average of two replicates at each of two nucleotide concentrations (see the Supporting Information).

To assess whether 300 μM nucleotide was a sufficiently high concentration to saturate Hsp104 and maximize oligomerization, sedimentation velocity experiments were repeated with 2 μM Hsp104 in the presence of 2 mM nucleotide (Figure 1B−E). In all cases, increasing the nucleotide concentration did not shift the dominant peak in the $c(s)$ distribution. Moreover, the magnitude of that peak, which reflects the relative concentration of that oligomer in solution, did not significantly change. Both *E. coli* ClpB and Hsp104 share structural domain organization, including the presence of an M domain. Our previous work indicates an $s_{20,w}$ of (17.6 ± 0.6) S for the ClpB hexamer, consistent with the dominant peaks observed in Figure 1A−E.[8] Thus, while definitive assignment of peaks to specific oligomers requires a multifaceted investigation beyond the scope of this study, the observed dominant peaks are likely hexameric Hsp104.

Table 1 shows the weight-average sedimentation coefficient, $\bar{s}_{20,w}$, for the dominant peak observed in the absence and presence of the nucleotides tested. Most strikingly, ATPγS binding clearly populates a hexamer that is hydrodynamically different from the hexamer populated with ADP, AMPPNP, AMPPCP, or no nucleotide.

The potentiated variant Hsp104A503S has enhanced disaggregation activity in numerous biological assays.[5] The mechanistic basis for this gain of function is unknown. To test whether Hsp104A503S has nucleotide-linked oligomerization properties different from those of wild-type Hsp104, we subjected the variant to sedimentation velocity experiments. As with wild-type Hsp104, hexamers populated in the presence of ATPγS are hydrodynamically different from those populated in the absence of nucleotide or in the presence of ADP, AMPPNP, or AMPPCP (Supporting Figure 1A−E and Supporting Table 1), though the difference between the ATPγS-bound and AMPPNP-bound states is smaller than that observed for the wild type. A similar observation was made for *E. coli* ClpB (Supporting Figure 2A−E and Supporting Table 1).

The analysis of the sedimentation velocity experiments presented in Figure 1 indicates that higher-order oligomers,

DOI: 10.1021/acs.biochem.7b00225
Biochemistry XXXX, XXX, XXX−XXX

consistent with hexamers, are observed under all conditions tested. The remaining question is whether these oligomers exhibit avid peptide binding. To test for peptide binding activity, we used a fluorescein-modified model polypeptide substrate termed FluNCysRepA50mer. Figure 2 shows the

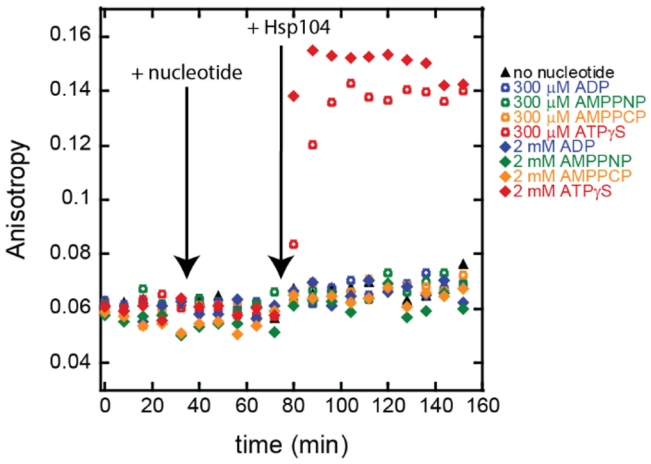

Figure 2. Fluorescence anisotropy measurements of FluNCysRepA50mer before and after subsequent additions of nucleotide and Hsp104 as indicated.

fluorescence anisotropy of a peptide solution upon addition of various nucleotides and Hsp104. The experiment begins with each sample containing only FluNCysRepA50mer. All time points of <40 min in Figure 2 report the anisotropy of the peptide alone, where $r = 0.060 \pm 0.004$ (replicate, $r = 0.069 \pm 0.004$).

Next, as shown in Figure 2 by an arrow indicating nucleotide addition, ADP, AMPPNP, AMPPCP, or ATPγS was added to each sample to a final nucleotide concentration of 300 μM. The anisotropy of the peptide in the presence of each nucleotide was within one standard deviation of the anisotropy of FluNCysRepA50mer alone, indicating that the nucleotide did not influence the observed anisotropy (Table 2).

Hsp104 was then added to each sample to a final concentration of 2 μM (Figure 2, arrow indicating Hsp104 addition). Strikingly, the anisotropy increased to 0.139 ± 0.002 for the sample containing 300 μM ATPγS. The increase in anisotropy indicates slower tumbling of FluNCysRepA50mer, consistent with peptide bound by the Hsp104 oligomer. In contrast, the anisotropy measurement did not significantly increase upon addition of Hsp104 in the presence of other nucleotides. As summarized in Table 2, the anisotropy measurements of the peptide in the presence of Hsp104 and ADP, AMPPNP, or AMPPCP were within one standard deviation of each other, and within one standard deviation of that of FluNCysRepA50mer in the presence of Hsp104 with no nucleotide, where $r = 0.068 \pm 0.004$ (replicate, $r = 0.072 \pm 0.002$). Inspection of the plot also reveals a minor upward trend in the anisotropy measurements taken after addition of Hsp104 under all conditions except ATPγS, indicating that there may be some small population of Hsp104 binding peptide under those conditions, consistent with substantially weaker affinity. These observations indicate that the ATPγS-bound Hsp104 oligomer has a unique competency for interactions with the polypeptide, not conferred by other nucleotides.

An alternative explanation is that 300 μM nucleotide is not sufficient to saturate Hsp104 binding. To test this possibility, the experiment was repeated using 2 mM nucleotide. The filled diamonds in Figure 2 illustrate that at 2 mM nucleotide, the anisotropy of the peptide remained constant (from ~40 to ~80 min). Table 2 lists the anisotropy measurements for the peptide under each of the 2 mM nucleotide conditions. Note that each measurement is within one standard deviation of the anisotropy value for the free peptide, where $r = 0.060 \pm 0.004$ (replicate, $r = 0.069 \pm 0.004$). Upon addition of Hsp104 to a final concentration of 2 μM, again only the ATPγS condition exhibited an increased anisotropy of 0.150 ± 0.005 that is consistent with binding polypeptide (Figure 2). Though a single representative time course is shown in Figure 2, the results are reproducible. The replicate time course is shown in Supporting Figure 3, while anisotropy values from the replicate are included in Table 2 for comparison. Both Hsp104A503S and ClpB were tested at nucleotide concentrations of 300 μM and 2 mM; the same trends were observed as for wild-type Hsp104 (Supporting Figure 4 and Supporting Tables 2 and 3).

We next sought to determine what conditions form a peptide–Hsp104 complex that is poised for ATP-dependent polypeptide translocation. We determined these conditions using a fluorescence stopped-flow assay, developed by our lab to study polypeptide translocation by ClpA and ClpB.[31−33] As schematized in Figure 3A, Hsp104, nucleotide, polypeptide

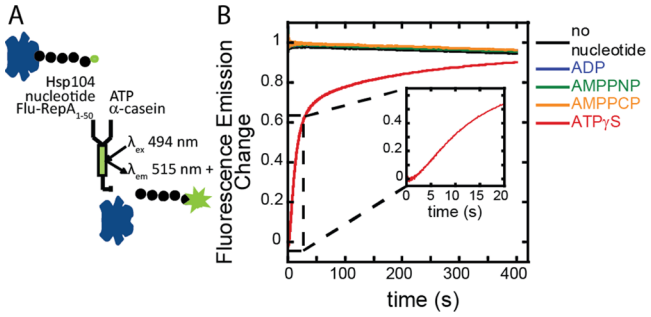

Figure 3. (A) Fluorescence stopped-flow reaction scheme and (B) time courses. Hsp104 and FluNCysRepA50mer were incubated in the presence of various nucleotides and then rapidly mixed with ATP and α-casein to test for the presence of a translocation-ready complex.

Table 2. Fluorescence Anisotropy for FluNCysRepA50mer[a]

	ADP (300 μM)	AMPPNP (300 μM)	AMPPCP (300 μM)	ATPγS (300 μM)	ADP (2 mM)	AMPPNP (2 mM)	AMPPCP (2 mM)	ATPγS (2 mM)
+ nucleotide	0.061 ± 0.002	0.062 ± 0.003	0.060 ± 0.002	0.059 ± 0.001	0.059 ± 0.003	0.055 ± 0.003	0.055 ± 0.003	0.059 ± 0.002
replicate	0.072 ± 0.001	0.071 ± 0.004	0.063 ± 0.003	0.070 ± 0.003	0.073 ± 0.004	0.066 ± 0.002	0.064 ± 0.003	0.065 ± 0.002
+ Hsp104	0.068 ± 0.003	0.067 ± 0.004	0.068 ± 0.003	0.139 ± 0.002	0.066 ± 0.003	0.062 ± 0.004	0.065 ± 0.002	0.150 ± 0.005
replicate	0.076 ± 0.002	0.076 ± 0.002	0.070 ± 0.002	0.190 ± 0.004	0.076 ± 0.002	0.073 ± 0.003	0.070 ± 0.002	0.178 ± 0.003

[a]The average and standard deviations were calculated as described in the Supporting Information.

DOI: 10.1021/acs.biochem.7b00225
Biochemistry XXXX, XXX, XXX−XXX

solutions were rapidly mixed with ATP and a protein trap to allow a single turnover of ATP-dependent translocation. The polypeptide substrate bound by Hsp104 exhibits quenched fluorescence (Supporting Figure 5) that is relieved upon Hsp104 dissociation.

As indicated in Figure 3B, the time courses for the samples incubated in the absence of nucleotide or with ADP, AMPPNP, or AMPPCP show an insignificant decrease in the intensity of the fluorescence signal over time, not indicative of ATP-driven events associated with a bound Hsp104−polypeptide complex. The time course for the ATPγS condition shows a low initial fluorescence, caused by fluorescence quenching in the bound complex (Supporting Figure 5), followed by an increase in fluorescence upon rapid mixing with ATP and protein trap. Note the presence of a lag phase (inset) indicating that assembled Hsp104 bound to the polypeptide in the presence of ATPγS takes at least two repeating kinetic steps before dissociating from the substrate, which is distinctly different from what we have reported for ClpB.[33] (This finding has prompted a thorough investigation of the Hsp104 translocation mechanism that is currently under way.) The stopped-flow results, like the fluorescence−anisotropy results, show that of the nucleotides tested only ATPγS supports avid binding of the polypeptide by Hsp104.

A prerequisite for resolving protein aggregates is binding a polypeptide substrate. Our sedimentation velocity work shows that there is a structural difference, resulting in a larger sedimentation coefficient and a smaller frictional coefficient for the ATPγS-bound Hsp104 hexamer compared to those of the apo, ADP-bound, AMPPNP-bound, or AMPPCP-bound Hsp104 hexamers (Table 1). The smaller frictional ratio, calculated in relation to a hydrated sphere of equivalent mass, indicates that the ATPγS-bound structure is more spherical than the other structures. The larger frictional ratio of the AMPPNP-bound structure reflects a less spherical shape, which is consistent with the asymmetric spiral hexamer observed by Yokom et al.[25] However, on the basis of the results reported here, that structure is not competent for avid polypeptide binding. The same general shape as that seen for the AMPPNP-bound Hsp104 oligomer is expected for the apo, ADP-bound, and AMPPCP-bound oligomers from our results.

Our anisotropy experiments show that, under the conditions tested, Hsp104 binds the unstructured polypeptide substrate only in the presence of ATPγS. Additionally, only ATPγS-bound Hsp104 forms a translocation-ready complex with a polypeptide in our stopped-flow experiments. Thus, only the unique structural conformation of ATPγS-bound Hsp104 is competent for avidly binding a polypeptide. Our findings are consistent with those of Lee et al., who showed that, because of differences in quaternary structure, AMPPNP, ADP, and the absence of a nucleotide do not promote binding of *T*ClpB to the polypeptide substrate, while ATPγS does.[11]

Studying ClpA, Farbman et al. described two possible peptide substrate-processing mechanisms as either an "alternating affinity" or a "constant affinity" model.[34] As each NBD cycles through ATP hydrolysis, the resulting conformational changes are associated with either a high or low affinity for the peptide. The coordination of these hydrolysis-driven conformational changes within the hexameric ring allows individual subunits to release a peptide substrate while the hexameric ring retains the substrate through multiple rounds of ATP hydrolysis.

Here, and in previous work, nucleotide analogues are used to approximate the structure of hydrolyzable ATP or a transition state along the reaction pathway from ATP to ADP-P_i. A single monomer within a hexamer that is bound by a transition state analogue likely reflects a physiologically relevant conformation along the reaction pathway. However, it is unlikely that all 12 NBDs within a hexamer would be synchronized with respect to hydrolysis, so a hexameric structure in which all protomers are ligated by the transition state analogue is not likely to be a conformational structure observed in the biological activity of the motor. Here, we see that when Hsp104 is saturated with ATPγS, a high-peptide affinity state is achieved. In contrast, when the motor is saturated by AMPPNP, AMPPCP, ADP, or no nucleotide, a low-peptide affinity state is induced.

Possible mechanistic implications proposed by Yokom et al. and Heuck et al. merit further investigation.[17,25] Hsp104 monomers within a hexamer may alternate between the conformations that give rise to planar and helical hexamers. Moreover, it has been reported that a mixture of ATP and ATPγS yields activity similar to that observed in the presence of cochaperone Hsp70.[26] Taken with our findings, this may indicate that binding by cochaperone Hsp70 is part of the mechanism of modulation between high- and low-peptide affinity states. Alternatively, a composite of the protomer conformation used to build up the planar and hexameric rings may be used in concert as the active hexamer cycles through ATP while engaged with a peptide substrate. Aggregates may also present multiple binding sites unlike soluble peptides that might increase binding affinity.

■ ASSOCIATED CONTENT

Supporting Information

The Supporting Information is available free of charge on the ACS Publications website at DOI: 10.1021/acs.biochem.7b00225.

Experimental procedures and additional supporting data (PDF)

■ AUTHOR INFORMATION

Corresponding Author

*E-mail: allucius@uab.edu.

ORCID

Aaron L. Lucius: 0000-0001-8636-5411

Funding

This work was supported by National Science Foundation Grant MCB-1412624 to A.L.L. and National Institutes of Health Grant R01GM099836 to J.S.

Notes

The authors declare no competing financial interest.

■ ACKNOWLEDGMENTS

We thank Peter Prevelige for confirmation of the ClpB sequence by mass spectrometry, Jingzhi Li and Bingdong Sha for protein preparation discussions, Amber Tariq for assistance with Hsp104 preparations, Woody Robbins and Kim Hardy for use of the French press, and Ethan Cagle for assistance with peptide labeling.

DOI: 10.1021/acs.biochem.7b00225
Biochemistry XXXX, XXX, XXX−XXX

REFERENCES

(1) Schirmer, E. C., Glover, J. R., Singer, M. A., and Lindquist, S. (1996) HSP100/Clp proteins: a common mechanism explains diverse functions. *Trends Biochem. Sci. 21*, 289.

(2) Neuwald, A. F., Aravind, L., Spouge, J. L., and Koonin, E. V. (1999) AAA$^+$: A Class of Chaperone-Like ATPases Associated with the Assembly, Operation, and Disassembly of Protein Complexes. *Genome Res. 9*, 27.

(3) Parsell, D. A., Kowal, A. S., Singer, M. A., and Lindquist, S. (1994) Protein disaggregation mediated by heat-shock protein Hspl04. *Nature 372*, 475.

(4) Shorter, J. (2008) Hsp104: A Weapon to Combat Diverse Neurodegenerative Disorders. *Neurosignals 16*, 63.

(5) Jackrel, M. E., DeSantis, M. E., Martinez, B. A., Castellano, L. M., Stewart, R. M., Caldwell, K. A., Caldwell, G. A., and Shorter, J. (2014) Potentiated Hsp104 Variants Antagonize Diverse Proteotoxic Misfolding Events. *Cell 156*, 170.

(6) Jackrel, M. E., and Shorter, J. (2014) Potentiated Hsp104 variants suppress toxicity of diverse neurodegenerative disease-linked proteins. *Dis. Models & Mech. 7*, 1175.

(7) Hattendorf, D. A., and Lindquist, S. L. (2002) Cooperative kinetics of both Hsp104 ATPase domains and interdomain communication revealed by AAA sensor-1 mutants. *EMBO J. 21*, 12.

(8) Lin, J., and Lucius, A. L. (2015) Examination of the dynamic assembly equilibrium for *E. coli* ClpB. *Proteins: Struct., Funct., Genet. 83*, 2008.

(9) Lin, J., and Lucius, A. L. (2016) Examination of ClpB Quaternary Structure and Linkage to Nucleotide Binding. *Biochemistry 55*, 1758.

(10) Lee, S., Sowa, M. E., Watanabe, Y. H., Sigler, P. B., Chiu, W., Yoshida, M., and Tsai, F. T. (2003) The Structure of ClpB: A Molecular Chaperone that Rescues Proteins from an Aggregated State. *Cell 115*, 229.

(11) Lee, S., Choi, J. M., and Tsai, F. T. (2007) Visualizing the ATPase Cycle in a Protein Disaggregating Machine: Structural Basis for Substrate Binding by ClpB. *Mol. Cell 25*, 261.

(12) DeSantis, M. E., Leung, E. H., Sweeny, E. A., Jackrel, M. E., Cushman-Nick, M., Neuhaus-Follini, A., Vashist, S., Sochor, M. A., Knight, M. N., and Shorter, J. (2012) Operational Plasticity Enables Hsp104 to Disaggregate Diverse Amyloid and Nonamyloid Clients. *Cell 151*, 778.

(13) Shorter, J., and Lindquist, S. (2004) Hsp104 Catalyzes Formation and Elimination of Self-Replicating Sup35 Prion Conformers. *Science 304*, 1793.

(14) Glover, J. R., and Lindquist, S. (1998) Hsp104, Hsp70, and Hsp40: A Novel Chaperone System that Rescues Previously Aggregated Proteins. *Cell 94*, 73.

(15) Schlee, S., Beinker, P., Akhrymuk, A., and Reinstein, J. (2004) A Chaperone Network for the Resolubilization of Protein Aggregates: Direct Interaction of ClpB and DnaK. *J. Mol. Biol. 336*, 275.

(16) Guo, F., Maurizi, M. R., Esser, L., and Xia, D. (2002) Crystal Structure of ClpA, an Hsp100 Chaperone and Regulator of ClpAP Protease. *J. Biol. Chem. 277*, 46743.

(17) Heuck, A., Schitter-Sollner, S., Suskiewicz, M. J., Kurzbauer, R., Kley, J., Schleiffer, A., Rombaut, P., Herzog, F., and Clausen, T. (2016) Structural basis for the disaggregase activity and regulation of Hsp104. *eLife 5*, e21516 DOI: 10.7554/eLife.21516.

(18) Wang, F., Mei, Z., Qi, Y., Yan, C., Hu, Q., Wang, J., and Shi, Y. (2011) Structure and mechanism of the hexameric MecA−ClpC molecular machine. *Nature 471*, 331.

(19) Wendler, P., Shorter, J., Snead, D., Plisson, C., Clare, D. K., Lindquist, S., and Saibil, H. R. (2009) Motor Mechanism for Protein Threading through Hsp104. *Mol. Cell 34*, 81.

(20) Lee, S., Sielaff, B., Lee, J., and Tsai, F. T. (2010) CryoEM structure of Hsp104 and its mechanistic implication for protein disaggregation. *Proc. Natl. Acad. Sci. U. S. A. 107*, 8135.

(21) Carroni, M., Kummer, E., Oguchi, Y., Wendler, P., Clare, D. K., Sinning, I., Kopp, J., Mogk, A., Bukau, B., and Saibil, H. R. (2014) Head-to-tail interactions of the coiled-coil domains regulate ClpB activity and cooperation with Hsp70 in protein disaggregation. *eLife 3*, e02481.

(22) Bösl, B., Grimminger, V., and Walter, S. (2005) Substrate Binding to the Molecular Chaperone Hsp104 and Its Regulation by Nucleotides. *J. Biol. Chem. 280*, 38170.

(23) Klosowska, A., Chamera, T., and Liberek, K. (2016) Adenosine diphosphate restricts the protein remodeling activity of the Hsp104 chaperone to Hsp70 assisted disaggregation. *eLife 5*, e15159.

(24) Effantin, G., Ishikawa, T., De Donatis, G. M., Maurizi, M. R., and Steven, A. C. (2010) Local and Global Mobility in the ClpA AAA+ Chaperone Detected by Cryo-Electron Microscopy: Functional Connotations. *Structure 18*, 553.

(25) Yokom, A. L., Gates, S. N., Jackrel, M. E., Mack, K. L., Su, M., Shorter, J., and Southworth, D. R. (2016) Spiral architecture of the Hsp104 disaggregase reveals the basis for polypeptide translocation. *Nat. Struct. Mol. Biol. 23*, 830.

(26) Doyle, S. M., Shorter, J., Zolkiewski, M., Hoskins, J. R., Lindquist, S., and Wickner, S. (2007) Asymmetric deceleration of ClpB or Hsp104 ATPase activity unleashes protein-remodeling activity. *Nat. Struct. Mol. Biol. 14*, 114.

(27) Doyle, S. M., Hoskins, J. R., and Wickner, S. (2007) Collaboration between the ClpB AAA+ remodeling protein and the DnaK chaperone system. *Proc. Natl. Acad. Sci. U. S. A. 104*, 11138.

(28) Doyle, S. M., Shastry, S., Kravats, A. N., Shih, Y. H., Miot, M., Hoskins, J. R., Stan, G., and Wickner, S. (2015) Interplay between E. coli DnaK, ClpB and GrpE during Protein Disaggregation. *J. Mol. Biol. 427*, 312.

(29) Lee, J., Kim, J. H., Biter, A. B., Sielaff, B., Lee, S., and Tsai, F. T. (2013) Heat shock protein (Hsp) 70 is an activator of the Hsp104 motor. *Proc. Natl. Acad. Sci. U. S. A. 110*, 8513.

(30) Zeymer, C., Barends, T. R., Werbeck, N. D., Schlichting, I., and Reinstein, J. (2014) Elements in nucleotide sensing and hydrolysis of the AAA+ disaggregation machine ClpB: a structure-based mechanistic dissection of a molecular motor. *Acta Crystallogr., Sect. D: Biol. Crystallogr. 70*, 582.

(31) Rajendar, B., and Lucius, A. L. (2010) Molecular Mechanism of Polypeptide Translocation Catalyzed by the Escherichia coli ClpA Protein Translocase. *J. Mol. Biol. 399*, 665.

(32) Miller, J. M., Lin, J., Li, T., and Lucius, A. L. (2013) E. coli ClpA Catalyzed Polypeptide Translocation Is Allosterically Controlled by the Protease ClpP. *J. Mol. Biol. 425*, 2795.

(33) Li, T., Weaver, C. L., Lin, J., Duran, E. C., Miller, J. M., and Lucius, A. L. (2015) Escherichia coli ClpB is a non-processive polypeptide translocase. *Biochem. J. 470*, 39.

(34) Farbman, M. E., Gershenson, A., and Licht, S. (2007) Single-Molecule Analysis of Nucleotide-Dependent Substrate Binding by the Protein Unfoldase ClpA. *J. Am. Chem. Soc. 129*, 12378.

DOI: 10.1021/acs.biochem.7b00225
Biochemistry XXXX, XXX, XXX−XXX

Supporting information for

Avidity for polypeptide binding by nucleotide-bound Hsp104 structures.

Experimental Procedures

Reagents and Buffers

All chemicals were reagent grade. All buffers were prepared with distilled, deionized water from a Purelab Ultra Genetic system (Evoqua, Warrendale, PA). Buffer HK150 contains 25 mM HEPES, pH 7.5 at 25 °C, 150 mM KCl, 10 mM $MgCl_2$, 2 mM 2-mercaptoethanol, and 10% (v/v) glycerol. ATP and ADP were purchased from Thermo Fisher Scientific (Waltham, MA). AMPPCP was purchased from Sigma-Aldrich (Darmstadt, Germany). ATPγS and AMPPNP were purchased from CalBiochem (La Jolla, CA).

Protein and Peptide

Hsp104 and Hsp104A503S were purified as described.[1,2] Protein concentrations are reported in monomer units. Hsp104 concentration was determined spectroscopically using ε280 = 32,500 M^{-1} cm^{-1}.

ClpB was expressed with an N-terminal His_6tag, followed by a TEV cleavage site for purification purposes. The mutagenesis was performed by GenScript (Piscataway, NJ). The PET-30a(+) plasmid was transformed into OneShot ® *E. coli* BL21(DE3) (Invitrogen) cells following the manufacturer's protocol. Protein was expressed in *E. coli* BL21(DE3) cells under *lac* operon control and with kanamycin resistance. Cell paste was suspended in cell lysis buffer [40 mM Tris, pH 7.5, at 4°C, 500 mM NaCl, 10% (w/v) sucrose, 20% (v/v) glycerol, 20 mM imidazole, 2 mM 2-mercaptoethanol]. Cells were lysed by two passes through a French press. DNase and RNase were added to the lysate and incubated with stirring at 4 °C for 15 minutes. Cell debris was pelleted by subjecting the lysate to centrifugation at 28,000 g in a ThermoScientific Fiberlite F14-6x250 rotor at 4 °C for 120 min. His_6ClpB was isolated by batch purification using GE Healthcare Bio-Sciences AB (Uppsala, Sweden) Ni SepharoseTM 6 Fast Flow charged media. The loose beads were incubated with the supernatant for 75 minutes at 4 °C with stirring and subsequently washed with 20-30 column volumes (where one column volume is defined as the volume of loose media used) nickel buffer 1 (40 mM Tris, pH 7.5 at 4 °C, 500 mM NaCl, 10% (v/v) glycerol, 20 mM imidazole, 2 mM 2-ME). The media, with bound protein, was then incubated with 1.5 CV of nickel buffer 2 (40 mM Tris, pH 7.5 at 4 C, 500 mM NaCl, 10% (v/v) glycerol, 500 mM imidazole, 2 mM 2-ME) for 30 minutes at 4 °C with rocking. The slurry was poured into a gravity column. The eluent was collected and the media was washed with an additional 6-7 column volumes of nickel buffer 2. His_6ClpB was dialyzed into digestion buffer (25 mM Tris pH 7.5 at 4 °C, 150 mM NaCl, 20% (v/v) glycerol, 500 uM EDTA, 2 mM 2-ME) in 15 KDa

cut off tubing. The His_6-tag on ClpB was cleaved by His_6 tagged Tobacco Etch Virus (TEV) protease (preparation described below) in a ratio of 27 mg His_6ClpB : 1 mg His_6-TEV. After digestion, the sample was dialyzed into nickel buffer 3 (40 mM Tris, pH 7.5 at 4 °C, 500 mM NaCl, 10% (v/v) glycerol, 500 mM imidazole, 2 mM 2-ME) and run over a GE Healthcare (Little Chalfont, UK) HisPrep FF 16/10 column. After washing with nickel buffer 3, ClpB from which the His_6 tag had been cleaved, was eluted with nickel buffer 1 (20 mM imidazole). His_6TEV, undigested His_6ClpB, and any remaining His_6 tags cleaved from the protein were eluted with nickel buffer 2 (500 mM imidazole). Note that the digested ClpB includes an N-terminal glycine residue that remains from the TEV cleavage site. The purity of ClpB was assessed to be greater than 95% by SDS/PAGE with Coomassie Brilliant Blue staining. Sequence was confirmed by mass spectrometry. ClpB was dialyzed into storage buffer (25 mM Tris pH 7.5 at 4 °C, 500 mM NaCl, 50% (v/v) glycerol, 500 uM EDTA, 2 mM 2-ME) in 50 kDa cut off tubing and stored at -80 °C until use. Protein concentrations are reported in monomer units using the extinction coefficient at 280 nm ε = 35,562 M^{-1} cm^{-1} determined in our lab by the method proposed by Edolhoch and later refined by Pace *et al.*[3,4]

TEV protease with an N-terminal His_6tag was expressed from glycerol stocks kindly provided by Dr Bingdong Sha, UAB. The *E. coli* cells were resistant to ampicillin and chloramphenicol. A starter culture grown at 37 °C was used to inoculate a 1 L growth that continued growing at 37 °C, 225 rpm until OD600 reached ~0.6. Expression was induced by adding 1 mM IPTG and the temperature was lowered to 20 °C while shaking (225 rpm) continued overnight. Cells were harvested by centrifugation (6.5 g cell paste from 1 L growth). Cell paste was suspended in cell lysis buffer [40 mM Tris, pH 7.5, at 4°C, 500 mM NaCl, 10% (w/v) sucrose, 5% (v/v) glycerol, 2 mM 2-mercaptoethanol]. Cells were lysed by sonication (12 cycles of 15 second pulse, 45 second rest). Cell debris was pelleted by subjecting the lysate to centrifugation at 28,000 g in a ThermoScientific Fiberlite F14-6x250 rotor at 4 °C for 90 min. His_6TEV protease was isolated by batch purification using GE Healthcare Bio-Sciences AB (Uppsala, Sweden) Ni SepharoseTM 6 Fast Flow charged media. The loose beads were incubated with the supernatant for 120 minutes at 4 °C with stirring and subsequently washed with 20-30 column volumes (where one column volume is defined as the volume of loose media used) nickel buffer 1. The media, with bound protein, was then incubated with 1.5 CV of nickel buffer 2 for 30 minutes at 4 °C with rocking. The slurry was poured into a gravity column. The eluent was collected and the media was washed with an additional 10 column volumes of elution buffer though the protein eluted within the first ~4 column volumes. The purity of His_6TEV protease was assessed to be greater than 95% by SDS/PAGE with Coomassie Brilliant Blue staining and the protein was determined to be ~ 1 mg/mL (40 mg total yield) based on absorbance at 280 nm and an extinction coefficient of ε = 32,290 M^{-1} cm^{-1}. His_6TEV protease was dialyzed into storage buffer in 15 kDa cut off tubing and stored at -80 °C until use, which is recommended to be within one year of purification (conversation with Dr Jingzhi Li, UAB).

The peptide, NCysRepA50mer (C MNQSFISDIL YADIESKAKE LTVNSNNTVQ PVALMRLGVF VPKPSKSKGE), was synthesized by CPC scientific (Sunnyvale, CA). Note that the cysteine residue was added for labeling purposes and is not part of the native RepA sequence. The subsequent 50 amino acids are the first 50 amino acids of the RepA sequence. The peptide was fluorescently modified

using fluorescein-5-maleimide, purchased from Life Technologies (Carlsbad, CA). The unmodified peptide was dissolved in 6 M guanidine hydrochloride, 20 mM HEPES, pH 7 at 25 °C and dialyzed against the same buffer. Fluorescein-5-maleimide was dissolved in 6 M guanidine hydrochloride, 20 mM HEPES, pH 7 at 25 °C to prepare a 30 mM solution. Tris(2-carboxyethyl)phosphine (TCEP) was dissolved in 6 M guanidine hydrochloride, 20 mM HEPES, pH 7 at 25 °C. These reagents were combined such that a 500 μL reaction mixture contained 100 μM peptide, 2 mM dye, and 1 mM TCEP. The labeling reaction proceeded for three hours at ambient temperature under partial vacuum. The labeled peptide was isolated using a GE Healthcare (Little Chalfont, UK) Superdex Peptide 10/300 GL column with absorbance monitored at 230 nm, 280 nm, and 495 nm. The column was run in an isocratic gradient of 6 M guanidine hydrochloride, 20 mM HEPES, pH 7 at 25 °C. The peptide was dialyzed into buffer HK150.The modified peptide is referred to as FluNCysRepA50mer.

α-Casein that was used as a protein trap in stopped flow experiments was purchased from Sigma-Aldrich (Darmstadt, Germany). The protein was dissolved in 6 M guanidine hydrochloride, 20 mM HEPES, pH 7 at 25 °C and dialyzed into HK150 using 1 kDa cut off tubing and stored at -20 °C until use. Protein concentrations were determined using the extinction coefficient at 280 nm $\varepsilon = 24{,}500\ M^{-1}\ cm^{-1}$.

Sedimentation Velocity Experiments

Sedimentation velocity experiments were performed on Hsp104 in a Beckman ProteomeLab XL-I analytical ultracentrifuge using the interference optical system (Beckman Coulter, Brea, CA). Experiments were carried out by loading 390 μL of sample and reference solutions into each corresponding sector of a 12 mm double sector Epon charcoal-filled centerpiece. Samples were subjected to an angular velocity of 40,000 rpm and scans were collected every 30 s at 25 °C.

Sample and reference solutions for each sedimentation velocity experiment were supplemented with identical concentrations of nucleotide to eliminate contributions from nucleotide to the signal. Protein samples were prepared by incubating 2 μM Hsp104 with either no nucleotide, or a fixed concentration of 300 μM or 2 mM of each of the four nucleotides tested: ATPγS, AMPPNP, ADP, and AMPPCP. Protein and reference solutions were prepared in HK150 and incubated for 2 hours at 25 °C before the first sedimentation scan was collected. Each experiment was performed with protein no older than two days from the time of dialysis.

Analysis of Sedimentation Velocity Experiments

Interference boundaries acquired from sedimentation velocity experiments were first corrected for time stamp errors[5,6] using REDATE Version 0.1.7 (Chad Brautigam, University of Texas Southwestern Medical Center). The corrected boundaries were then analyzed using SEDFIT version 14.4f (Peter Schuck, NIH) as previously described.[7,8] The data were analyzed between the meniscus plus 0.01 cm and 6.7 cm to minimize the contribution from gradients of glycerol and nucleotide to the sedimentation boundaries.[7] The weight

average sedimentation coefficients reported in Table 1 were obtained by integrating the c(s) distributions over the range of $s_{20,w}$ ~14 – 20 S. For each nucleotide, the sedimentation coefficients obtained from the two nucleotide concentrations tested in duplicate were averaged. The corresponding standard deviations are reported in Table 1. All sedimentation coefficients, s, are reported as $s_{20,w}$ by correcting s to the standard solution condition of water at 20 °C, as previously described, using Eq. (S1):[7,9]

$$s_{20,w} = \frac{\left(1-\rho_{20,w}\bar{v}\right)}{\left(1-\rho\bar{v}\right)} \cdot \frac{\eta}{\eta_{20,w}} \cdot s \qquad \text{(S1)}$$

where ρ is the density of the buffer, $\bar{v}$ is partial specific volume of the protein, and η is viscosity. The partial specific volume for Hsp104 was calculated to be 0.7398 mL g^{-1} from the protein sequence using Sednterp[10] (David Hayes, Magdalen College, Tom Laue, University of New Hampshire, and John Philo, Alliance Protein Laboratories). A correction of $\Delta\bar{v}$ = +0.0033 mL g^{-1} (Eq. (S2))[11] was added to obtain a final value of $\bar{v}$ = 0.7431 mL g^{-1}, that accounts for changes in hydration due to the presence of 10 % glycerol in the buffer used here, as previously done by us to examine the hydrodynamics of ClpA[12] and ClpB[7].

$$\frac{\Delta\bar{v}}{\Delta[\text{glycerol}]\%(\text{v/v})} = \left(3.33 \pm 0.38\right) \times 10^{-4} \text{ mL g}^{-1} \qquad \text{(S2)}$$

Analysis of Frictional Ratios

The ratio of the frictional coefficient (*f*) of Hsp104 relative to the frictional coefficient of a hydrated sphere of equal mass (f_0), can be used to gain insight into how the sedimentation coefficient correlates to structure. Frictional coefficient ratios (f/f_0) were determined using weight average sedimentation coefficients for Hsp104 (Table 1). The frictional ratios were calculated using the measured $s_{20,w}$ as done previously by us to investigate the self-assembly of ClpA[13] using Eq. (S3):

$$\frac{f}{f_0} = \left(\frac{M^2\left(1-\bar{v}\rho\right)^3}{162\pi^2 S_{20,w}^3 \eta^3 N_A^2 (\bar{v} + \delta\bar{v}_{H_2O})} \right)^{\frac{1}{3}} \qquad \text{(S3)}$$

where *f* is the frictional coefficient for Hsp104, f_0 is the frictional coefficient of a hydrated sphere of equivalent mass, *M* is the molecular weight of Hsp104 (102,648 g/mol), N_A is Avogadro's number, and δ is the degree of hydration of Hsp104 (grams of water bound per gram of Hsp104). The degree of hydration was determined from sequence using Sednterp to be 0.4342 g. As done previously by us, a correction

was applied to the degree of hydration value to account for the observation that only 70 % of the degree of hydration calculated using the Kuntz method is associated with a folded protein.[13,14] After this correction is applied, the degree of hydration of Hsp104 is approximated to be 0.3039 g of water bound per macromolecule. The resulting values for the frictional ratio obtained for Hsp104 in the presence of each nucleotide condition tested are summarized in Table 1.

Fluorescence Anisotropy

Steady state fluorescence anisotropy was monitored by exciting fluorescein at 494 nm and observing emission at 515 nm in a Fluorolog-3 spectrophotometer (HORIBA Jobin Yovin, Edison, NJ) as previously described.[15] Measurements were made with FluNCysRepA50mer alone, then upon subsequent additions of various nucleotides, and finally addition of Hsp104. Final concentrations were 20 nM FluNCysRepA50mer, either 300 μM or 2 mM nucleotide, and 2 μM Hsp104. Note that anisotropy is not concentration dependent so the minor changes in concentration due to sequential additions of components does not contribute to the anisotropy signal. Experiments were performed at 25 °C in buffer HK150.

For each data set presented, the average and standard deviations are reported as follows. The anisotropy value for peptide alone is the average of all time points from all samples which contain only peptide. For example, the anisotropy value $r = 0.060 \pm 0.004$ reported in the main text for free peptide in buffer is the average and standard deviation of 50 total time points, ten time points from the "no nucleotide" sample, Figure 2 black triangles (from time 0 to 80 minutes) and five time points from each of the eight samples to which nucleotide was subsequently added (time 0 to 40 minutes). The "+ nucleotide" values reported in Table 2 are the average and standard deviation of the five time points from 40 to 80 minutes from each sample containing nucleotide. The agreement of these values across nucleotide concentration (300 μM and 2 mM) and nucleotide identity (ADP, AMPPNP, AMPPCP, ATPγS) demonstrates that the anisotropy of the peptide is not affected by the presence of nucleotide. The "+ Hsp104" values reported in Table 1 are the average and standard deviation of the ten time points from 80 to 160 minutes for each nucleotide condition, with the exception of the ATPγS conditions. Because the time courses for ATPγS include an increase in the anisotropy value over the first two anisotropy measurements after addition of protein, the average and standard deviation of the final eight time points (90 to 160 minutes) are reported, representing the final anisotropy of the complex formed by peptide and Hsp104 in the presence of ATPγS. The calculations for average and standard deviation were conducted in the same manner for the Hsp104A503S and ClpB results reported in Supporting Figure 4 and Supporting Tables 3 and 4. The averages and standard deviations for a replicate of the Hsp104 WT anisotropy data reported in Supporting Figure 3 and Table 2 follow the same strategy.

Fluorescence Stopped Flow – Raw Fluorescence

Fluorescence stopped flow experiments were performed using an Applied Photophysics (Leatherhead, U.K.) SX20 stopped-flow fluorimeter as previously described.[16-18] These experiments were conducted at 25 °C in buffer HK150. Fluorescence of the fluorescein on FluNCysRepA50mer was observed by excitation at 494 nm with emission observed above 515 nm using a 515 nm long-pass filter.

The first syringe contained 2 μM Hsp104, 300 μM nucleotide (or no nucleotide), and 20 nM FluNCysRepA50mer (see Figure 3 A). In the motor protein-peptide complex, the fluorescence of the fluorescein is quenched (see Figure S5B and associated description). The second syringe contained 10 mM ATP and 20 μM α-casein. The α-casein serves as a protein trap to bind any free Hsp104 upon mixing, maintaining single-turnover reaction conditions with respect to the Hsp104-polypeptide complex. The contents of each syringe were incubated for one hour at 25 °C prior to the experiment. The change in fluorescence emission was monitored over 400 seconds.

Fluorescence Stopped-Flow – Anisotropy and Total Fluorescence

Fluorescence stopped flow experiments were performed using an Applied Photophysics (Leatherhead, U.K.) SX20 stopped-flow fluorimeter with the fluorescence polarisation accessory, two 515 nm long-pass filters and two R6095 photomultiplier tubes. These experiments were conducted at 25 °C in buffer HK150. FluNCysRepA50mer was excited at 494 nm. The first syringe contained 2 μM Hsp104 and 300 μM ATPγS. The second syringe contained 20 nM FluNCysRepA50mer. The contents of each syringe were incubated for one hour at 25 °C prior to the experiment. Upon rapid mixing, anisotropy and total fluorescence were simultaneously observed for 1800 s.

Additional Results

Analytical Ultracentrifugation Results with Hsp104A503S and ClpB

Sedimentation velocity experiments were performed on the Hsp104 potentiated variant, Hsp104A503S, and the bacterial homologue of Hsp104, *E. coli* ClpB. These experiments were performed identically to the sedimentation velocity experiments described in the main text, with the appropriate protein substitution. The resulting c(s) distributions for Hsp104A503S and ClpB are shown in Supporting Figures 1 and 2, respectively. The resulting weight average sedimentation coefficient for the largest boundaries observed for Hsp104A503S and ClpB are summarized in Supporting Table 1.

Similarly to Hsp104, the predominant c(s) distribution observed for Hsp104A503S in the absence of nucleotide (Supporting Table 1) has a weight average sedimentation coefficient of ~16. S. The dominant c(s) distribution observed for Hsp104A503S in the presence of ADP (blue traces), AMPPNP (green traces), and AMPPCP (orange traces), exhibits a weight average sedimentation coefficient ranging between ~ (15.8 – 16.5) S. By comparison to the analogous experiments with Hsp104, this is consistent with the formation of hydrodynamically similar Hsp104A503S hexamers in the absence of nucleotide as well as in the presence of ADP, AMPPNP, and AMPPCP. In contrast, when the sedimentation velocity experiments are carried out on Hsp104A503S in the presence of ATPγS (red

traces), the weight average sedimentation coefficient of the predominant distribution observed was ~ (17.0 – 17.2) S. This again is consistent with our observations for wild-type Hsp104, suggesting that Hsp104A503S hexamers populated in the presence of ATPγS are hydrodynamically different from those observed in the absence of nucleotide or in the presence of the other nucleotides tested. Notably, the sedimentation coefficient in the presence of 2 mM AMPPNP (dark green trace in Supporting Figure 1 C) is higher than observed in all other conditions except with ATPγS. While visual inspection may suggest that this represents an oligomer consistent with the ATPγS bound oligomer, the sedimentation coefficient is half a Svedberg unit lower than the oligomer observed in the presence of ATPγS indicating that there are still notable differences between the structures. Furthermore, the anisotropy experiments discussed below (Supporting Figure 4) demonstrate that the Hsp104A503S oligomer bound by AMPPNP does not avidly bind peptide.

Interestingly, the predominant c(s) distribution observed for 2 μM ClpB in the absence of nucleotide (Supporting Figure 2 A) was not the largest oligomer in all cases. Here, we use 200 mM NaCl for consistency with our other ClpB experiments, reported here and elsewhere. We have previously shown that at 200 mM NaCl ClpB resides in a distribution of oligomers in which the hexamer is not the predominant species. [7] In order to compare the sedimentation coefficient values for the largest species that could be populated both in the absence and presence of the nucleotides tested, weight average sedimentation coefficient for the boundary with the greatest sedimentation coefficient from each c(s) distribution shown in Supporting Figure 2, was determined and summarized in Supporting Table 1. As with Hsp104 WT and A503S, a hydrodynamically different state for ClpB was observed only in the presence of ATPγS, compared to all other conditions tested.

Reproducibility of anisotropy binding observations

Supporting Figure 3 represents a complete replicate of Figure 2 of the main text. This was accomplished by making up all of the reagents fresh and doing the experiment again on another day. The anisotropy values, with error, are reported in Table 2 of the main text. As can be seen, the data are reproducible.

Potentiated variant Hsp104A503S and bacterial homologue of Hsp104WT *E. coli* ClpB bind peptide avidly only in the presence of ATPγS

Hsp104A503S is a variant with increased disaggregation activity and efficacy against disease models relative to wild type Hsp104.[2,19] We sought to determine whether this enhanced activity was due to differences in polypeptide binding. For example, could Hsp104A503S bind peptide substrate under conditions where Hsp104 could not? To test for this possibility, Hsp104A503S was used in a steady state anisotropy binding experiment identical to that presented in Figure 2 of the main text.

Supporting Figure 4, panel A, shows the anisotropy of the peptide over time. As in the primary text, the experiment begins with each sample containing only FluNCysRepA50mer in buffer HK150. All time points below 40 minutes in Supporting Figure 4A report the

anisotropy of FluNCysRepA50mer in the absence of nucleotide, and also in the absence of Hsp104A503S. The fluorescein modified polypeptide exhibits an anisotropy of $r = 0.072 \pm 0.003$. Next, as shown in Supporting Figure 4, panel A, by an arrow indicating nucleotide addition at 38 minutes, ADP (blue), AMPPNP (green), AMPPCP (orange), or ATPγS (red) was added to each sample such that the final concentration was 300 μM nucleotide (open circles) or 2 mM nucleotide (filled diamonds). As summarized in the top row of Supporting Table 2, the anisotropy measurement for the peptide in the presence of each nucleotide was within one standard deviation of the anisotropy measurement for FluNCysRepA50mer alone.

Hsp104A503S was then added to each sample, as indicated in the figure, to a final concentration of 2 μM. As observed with the wild-type Hsp104 experiments, there was no significant change in the anisotropy of the peptide in the presence of either 300 μM or 2 mM ADP (blue), AMPPNP (green), AMPPCP (orange). As summarized in the bottom row of Supporting Table 2, the anisotropy measurements of the peptide in the presence of Hsp104A503S and ADP, AMPPNP, or AMPPCP were within one standard deviation of each other, and also within one standard deviation of the measurement for FluNCysRepA50mer in the presence of Hsp104A503S with no nucleotide, $r = 0.073 \pm 0.002$. In sharp contrast to the other nucleotides, and consistent with the observations made using wild-type Hsp104, the anisotropy increased to $r = 0.209 \pm 0.004$ in the presence of 300 μM ATPγS, and $r = 0.213 \pm 0.003$ in the presence of 2 mM ATPγS. The increase in anisotropy indicates that FluNCysRepA50mer is bound by the Hsp104A503S oligomer, resulting in the slower tumbling. In comparison to the time course collected for wild-type Hsp104, the magnitude and rate of change in anisotropy upon peptide binding by Hsp104A503S are both greater. This suggests that there may be some subtle differences in binding affinity of the wild-type or variant for this peptide which invite further investigation. The primary observation, however, is that both wild-type Hsp104 and Hsp104A503S require ATPγS in order to avidly bind this model unstructured peptide and the other nucleotides examined cannot substitute.

E. coli ClpB is the bacterial homologue of yeast Hsp104.[20] ClpB and Hsp104 are similar in both structure and function, though Hsp104 is able to disaggregate more complex amyloid aggregates while ClpB cannot.[21] Recent investigation of the molecular mechanism of ClpB revealed that it is a non-processive translocase, in contrast with the prevailing model in the field of "threading" or processive polypeptide translocation.[16,22-24] We sought to determine whether these homologous proteins have the same requirements for peptide binding by performing the anisotropy experiments described above using ClpB.

Supporting Figure 4, panel B, shows the anisotropy of the peptide over time. The experiment begins with each sample containing only FluNCysRepA50mer in buffer HK150. All time points below 40 minutes in Supporting Figure 4B report the anisotropy of FluNCysRepA50mer in the absence of nucleotide, and also in the absence of ClpB. The fluorescein modified polypeptide exhibits an anisotropy of $r = 0.060 \pm 0.003$. Next, as shown in Supporting Figure 4, panel B, by an arrow indicating nucleotide addition at 38 minutes,

ADP (blue), AMPPNP (green), AMPPCP (orange), or ATPγS (red) was added to each sample such that the final concentration was 300 μM nucleotide (open circles) or 2 mM nucleotide (filled diamonds). As summarized in the top row of Supporting Table 3, the anisotropy measurement for the peptide in the presence of each nucleotide was within one standard deviation of the anisotropy measurement for FluNCysRepA50mer alone.

ClpB was then added to each sample, as indicated in Supporting Figure 4, panel B, to a final concentration of 2 μM. As observed with both the wild-type and variant Hsp104 experiments, there was no significant change in the anisotropy of the peptide in the presence of either 300 μM or 2 mM ADP (blue), AMPPNP (green), AMPPCP (orange). As summarized in the bottom row of Supporting Table 3, the anisotropy measurements of the peptide in the presence of ClpB and ADP, AMPPNP, or AMPPCP were within one standard deviation of each other, and also within one standard deviation of the measurement for FluNCysRepA50mer in the presence of Hsp104A503S with no nucleotide, $r = 0.061 \pm 0.002$. In sharp contrast to the other nucleotides, and consistent with the observations made using wild type and variant Hsp104, the anisotropy increased to $r = 0.10 \pm 0.01$ in the presence of 300 μM ATPγS, and $r = 0.133 \pm 0.006$ in the presence of 2 mM ATPγS. Like Hsp104, ClpB only binds peptide in the presence of ATPγS. There are, however, notable differences in the time course for ClpB as compared with the Hsp104 and Hsp104A503S experiments. The increase in anisotropy is slower when the motor protein studied is ClpB. In fact, the 300 μM ATPγS trace (red open circles) appears to still be increasing even 75 minutes after addition of the final component. The time courses generated in the presence of low (300 μM, red open circles) or high (2 mM, red filled diamonds) ATPγS concentrations are notably different. These findings suggest that ClpB binding of the polypeptide substrate is slower, and more dependent upon the ATPγS concentration than its homologue Hsp104.

Binding of FluNCysRepA50mer Results in Quenching of Fluorescein Fluorescence

Nucleotide bound Hsp104 was rapidly mixed with fluorescently modified polypeptide to determine if binding of Hsp104 to polypeptide substrates induces fluorescence changes in addition to the observed anisotropy change. To this end, a solution of Hsp104 and ATPγS was rapidly mixed with a solution of FluNCysRepA50mer as schematized in Supporting Figure 5, panel A; the resulting anisotropy and total fluorescence time courses are displayed in Supporting Figure 5, panel B. The red trace indicates an increase in anisotropy, consistent with the observations in Figure 2. (Note that the L format of the fluorimeter and the T format of the fluorescence stopped-flow give rise to different anisotropy values. In either format, an increase in anisotropy upon binding of Hsp104 to FluNCysRepA50mer is observed.) The simultaneous total fluorescence time course (black trace) shows a decrease in fluorescence, or fluorescence quenching, upon binding. This finding allows us to monitor fluorescence of the pre-bound complex in a translocation assay with an increase in fluorescence indicating dissociation of Hsp104 from polypeptide substrate shown in Figure 3. This is the same approach employed in our studies of the translocation mechanisms of ClpB and ClpA.

Supporting References

(1) Desantis, M. E.; Sweeny, E. A.; Snead, D.; Leung, E. H.; Go, M. S.; Gupta, K.; Wendler, P.; Shorter, J. *J Biol Chem* **2014**, *289*, 848.

(2) Jackrel, M. E.; DeSantis, M. E.; Martinez, B. A.; Castellano, L. M.; Stewart, R. M.; Caldwell, K. A.; Caldwell, G. A.; Shorter, J. *Cell* **2014**, *156*, 170.

(3) Edelhoch, H. *Biochemistry* **1967**, *6*, 1948.

(4) Pace, C. N.; Vajdos, F.; Fee, L.; Grimsley, G.; Gray, T. *Protein Sci* **1995**, *4*, 2411.

(5) Zhao, H.; Ghirlando, R.; Piszczek, G.; Curth, U.; Brautigam, C. A.; Schuck, P. *Analytical biochemistry* **2013**, *437*, 104.

(6) Ghirlando, R.; Balbo, A.; Piszczek, G.; Brown, P. H.; Lewis, M. S.; Brautigam, C. A.; Schuck, P.; Zhao, H. *Analytical biochemistry* **2013**, *440*, 81.

(7) Lin, J.; Lucius, A. L. *Proteins* **2015**, *83*, 2008.

(8) Lin, J.; Lucius, A. L. *Biochemistry* **2016**, *55*, 1758.

(9) Schuck, P. *Biophys J* **1998**, *75*, 1503.

(10) Laue, T. M., Shah, B.D., Ridgeway, T.M., Pelletier, S.L. In *Analytical Ultracentrifugation in Biochemistry and Polymer Science*; S.E. Harding, A. J. R., J.C. Horton, Ed.; Royal Society of Chemistry: Cambridge, 1992.

(11) Cole, J. L. *Biochemistry* **1996**, *35*, 15601.

(12) Veronese, P. K.; Lucius, A. L. *Biochemistry* **2010**, *49*, 9820.

(13) Veronese, P. K.; Stafford, R. P.; Lucius, A. L. *Biochemistry* **2009**, *48*, 9221.

(14) Kuntz, I. D. *J Am Chem Soc* **1971**, *93*, 516.

(15) Li, T.; Lucius, A. L. *Biochemistry* **2013**, *52*, 4941.

(16) Li, T.; Weaver, C. L.; Lin, J.; Duran, E. C.; Miller, J. M.; Lucius, A. L. *The Biochemical journal* **2015**, *470*, 39.

(17) Lucius, A. L.; Miller, J. M.; Rajendar, B. *Methods Enzymol* **2011**, *488*, 239.

(18) Rajendar, B.; Lucius, A. L. *J Mol Biol* **2010**, *399*, 665.

(19) Jackrel, M. E.; Shorter, J. *Dis Model Mech* **2014**, *7*, 1175.

(20) Parsell, D. A.; Sanchez, Y.; Stitzel, J. D.; Lindquist, S. *Nature* **1991**, *353*, 270.

(21) DeSantis, M. E.; Leung, E. H.; Sweeny, E. A.; Jackrel, M. E.; Cushman-Nick, M.; Neuhaus-Follini, A.; Vashist, S.; Sochor, M. A.; Knight, M. N.; Shorter, J. *Cell* **2012**, *151*, 778.

(22) Weibezahn, J.; Tessarz, P.; Schlieker, C.; Zahn, R.; Maglica, Z.; Lee, S.; Zentgraf, H.; Weber-Ban, E. U.; Dougan, D. A.; Tsai, F. T.; Mogk, A.; Bukau, B. *Cell* **2004**, *119*, 653.

(23) Watanabe, Y. H.; Nakazaki, Y.; Suno, R.; Yoshida, M. *The Biochemical journal* **2009**, *421*, 71.

(24) Nakazaki, Y.; Watanabe, Y. H. *Genes Cells* **2014**, *19*, 891.

Supporting Figures

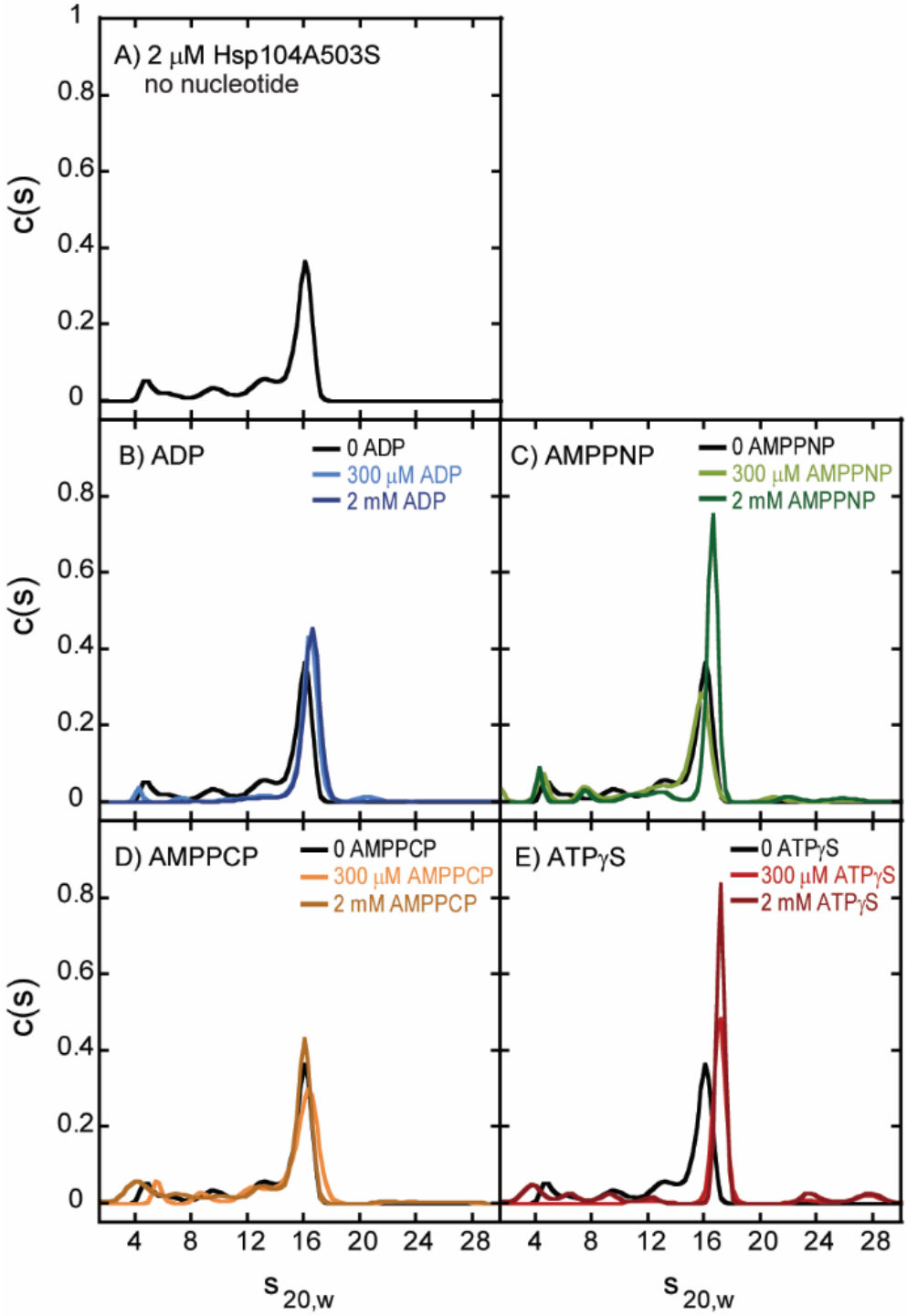

Supporting Figure 1. Sedimentation velocity c(s) distributions of Hsp104A503S in the absence and presence of nucleotides. Sedimentation velocity experiments were performed on 2 μM Hsp104 in the absence (A) and presence of ADP, AMPPNP, AMPPCP, or ATPγS (B-E).

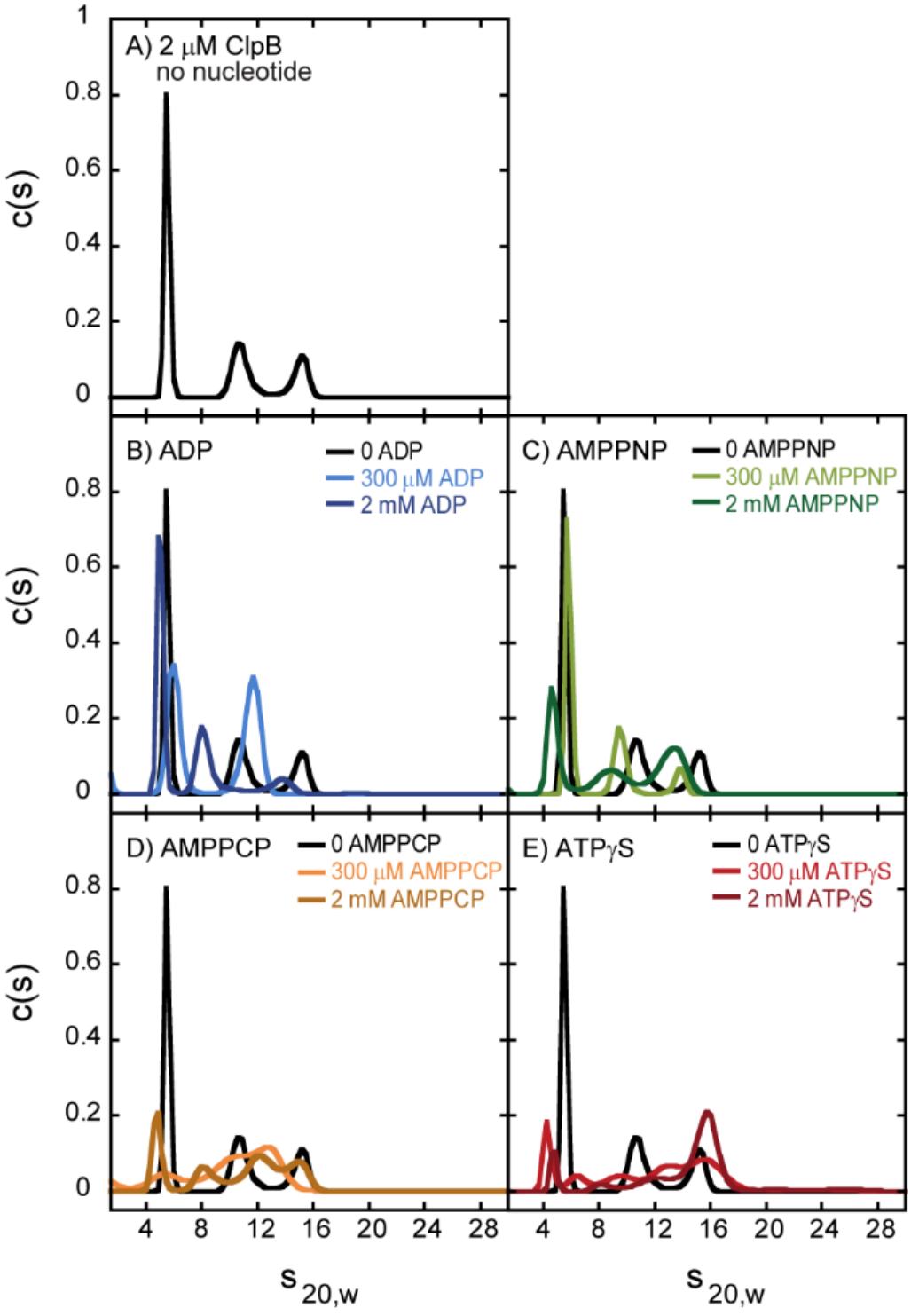

Supporting Figure 2. Sedimentation velocity c(s) distributions of ClpB in the absence and presence of nucleotides. Sedimentation velocity experiments were performed on 2 μM ClpB in the absence (A) and presence of ADP, AMPPNP, AMPPCP, or ATPγS (B-E).

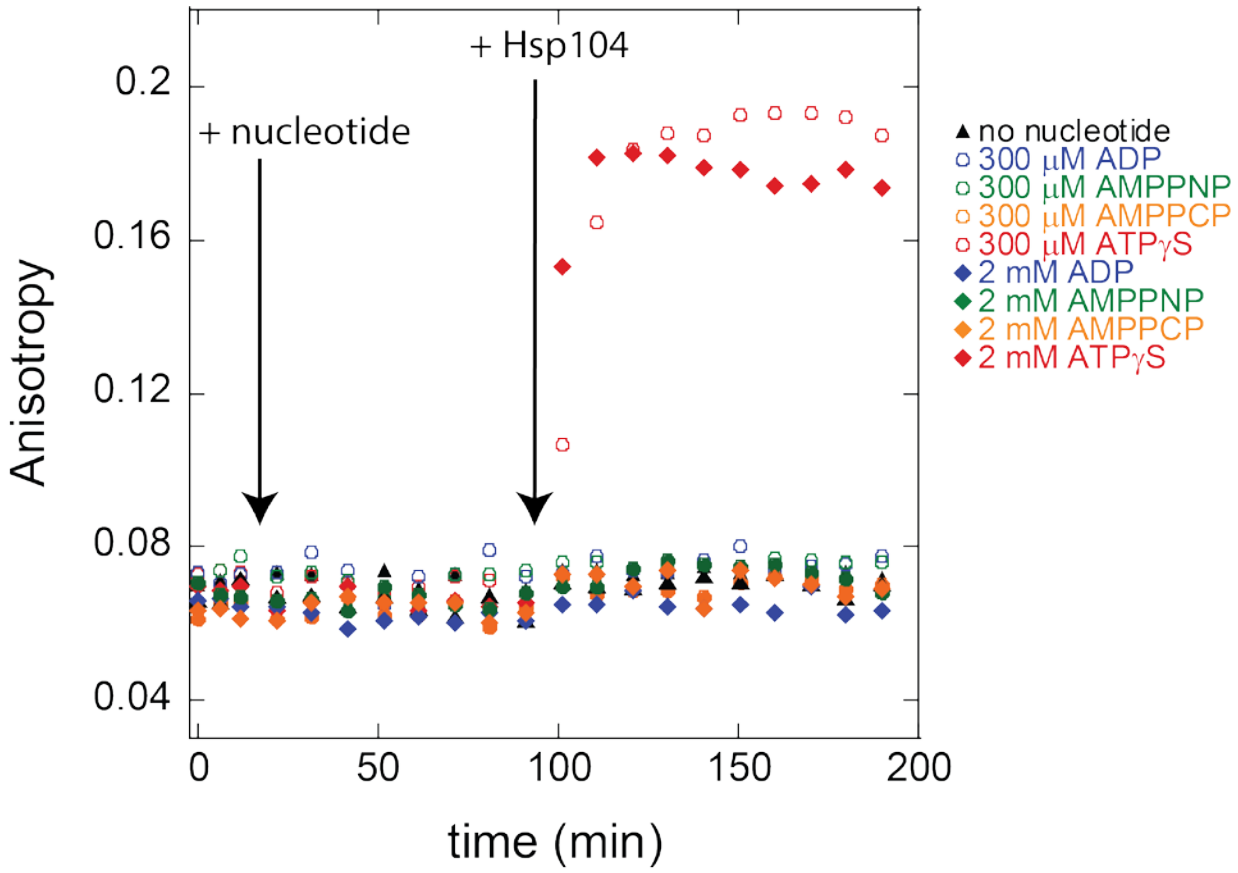

Supporting Figure 3. Representative replicate of fluorescence anisotropy measurements of Flu-NCysRepA50mer before and after subsequent additions of nucleotide and Hsp104 where indicated.

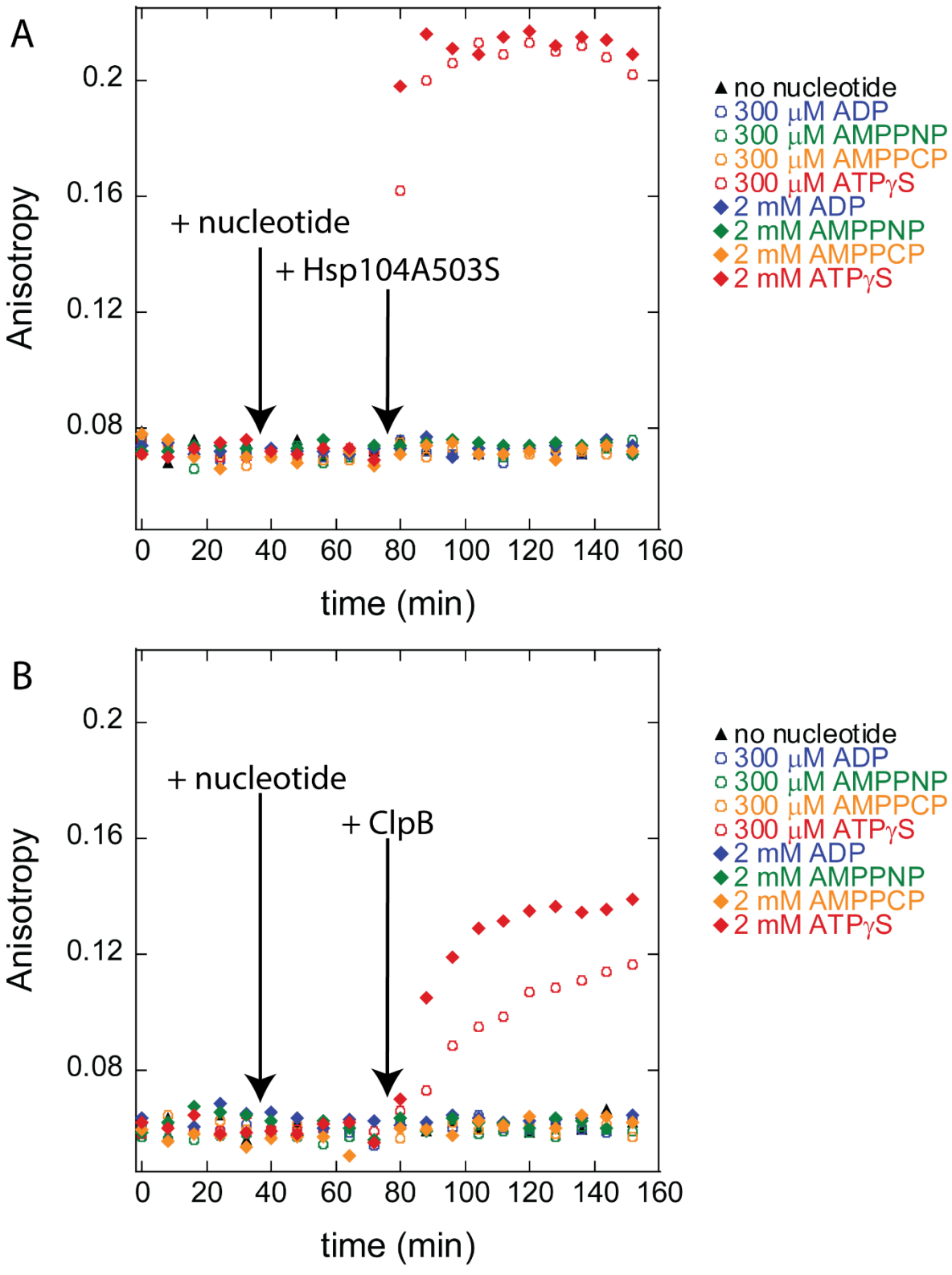

Supporting Figure 4. Fluorescence anisotropy measurements of Flu-NCysRepA50mer before and after subsequent additions of nucleotide and (A) Hsp104A503S or (B) ClpB where indicated.

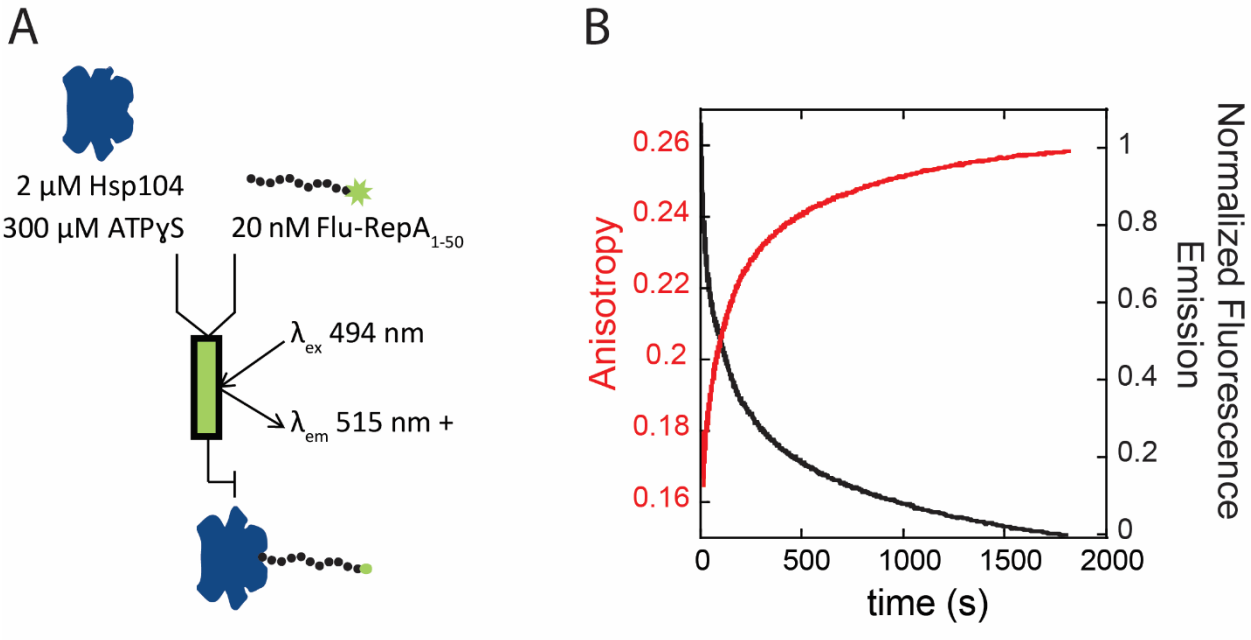

Supporting Figure 5. Binding experiment reaction schematic (A) and fluorescence anisotropy and total fluorescence time courses (B). Hsp104 and ATPγS were rapidly mixed with Flu-NCysRepA50mer. Fluorescence anisotropy and total fluorescence were observed simultaneously.

Supporting Table 1. Hsp104A503S and ClpB largest c(s) distribution

Condition	Hsp104A503S $s_{20,w}$ (S)	ClpB $s_{20,w}$ (S)
No nucleotide	16.014 ± 0.005	15.16 ± 0.02
300 μM ADP	16.414 ± 0.003	11.89 ± 0.01
2 mM ADP	16.465 ± 0.003	13.74 ± 0.03
300 μM AMPPNP	15.749 ± 0.004	13.86 ± 0.03
2 mM AMPPNP	15.930 ± 0.004	13.27 ± 0.01
300 μM AMPPCP	16.029 ± 0.008	12.98 ± 0.01
2 mM AMPPCP	15.930 ± 0.004	14.45 ± 0.01
300 μM ATPγS	17.041 ± 0.003	15.96 ± 0.01
2 mM ATPγS	17.165 ± 0.003	15.848 ± 0.004

Standard deviations were determined from Monte Carlo analysis in SedFit.

Supporting Table 2. Fluorescence anisotropy of FluNCysRepA50mer with Hsp104A503S

	ADP	AMPPNP	AMPPCP	ATPγS	ADP	AMPPNP	AMPPCP	ATPγS
	300 μM	300 μM	300 μM	300 μM	2 mM	2 mM	2 mM	2 mM
+ nucleotide	0.0708 ± 0.0007	0.071 ± 0.002	0.0695 ± 0.0008	0.0720 ± 0.0006	0.072 ± 0.001	0.073 ± 0.002	0.070 ± 0.003	0.071 ± 0.002
+ Hsp104 A503S	0.072 ± 0.002	0.073 ± 0.002	0.072 ± 0.001	0.209 ± 0.004	0.074 ± 0.002	0.074 ± 0.001	0.072 ± 0.002	0.213 ± 0.003

The averages and standard deviations were calculated as described in Experimental Procedures.

Supporting Table 3. Fluorescence anisotropy of FluNCysRepA50mer with ClpB

	ADP	AMPPNP	AMPPCP	ATPγS	ADP	AMPPNP	AMPPCP	ATPγS
	300 μM	300 μM	300 μM	300 μM	2 mM	2 mM	2 mM	2 mM
+ nucleotide	0.058 ± 0.003	0.057 ± 0.002	0.059 ± 0.002	0.060 ± 0.001	0.063 ± 0.002	0.060 ± 0.003	0.055 ± 0.003	0.059 ± 0.003
+ ClpB	0.061 ± 0.002	0.060 ± 0.002	0.060 ± 0.001	0.10 ± 0.01	0.063 ± 0.001	0.063 ± 0.002	0.062 ± 0.002	0.133 ± 0.006

The averages and standard deviations were calculated as described in Experimental Procedures.